When ternary PdCuP alloys meet ultrathin nanowires: Synergic boosting of catalytic performance in ethanol electrooxidation

Hao Lv[a], Lizhi Sun[a], Dongdong Xu[a,*], Yanhang Ma[b], Ben Liu[a,*]

[a] *Jiangsu Key Laboratory of New Power Batteries, Collaborative Innovation Center of Biomedical Functional Materials, School of Chemistry and Materials Science, Nanjing Normal University, Nanjing 210023, China*
[b] *School of Physical Science and Technology, ShanghaiTech University, Shanghai 201210, China*

ABSTRACT

Noble metal-phosphorus (NMP) alloys have received special attention in the electrocatalysis. Despite a few efforts, the fabrication of anisotropic multicomponent NMPs is largely unsuccessful. Here we develop a facile yet general surfactant-directed aqueous synthesis for one-dimensional (1D) ternary PdCuP alloy nanowires (NWs), and demonstrate their structural and compositional synergy in promoting catalytic performance towards ethanol electrooxidation. Anisotropic PdCuP NWs with an ultrathin diameter of 2.5 nm and ultralong length of hundreds of nanometers are synthesized *via* in-the-columnar epitaxial growth of crystalline alloys along columnar assemblies of amphiphilic dioctadecyldimethylammonium chloride (DODAC) by NaH_2PO_2 as the reducing agent and P source simultaneously. This protocol is also synthetically universal, enables the controllability in tuning the P contents and elemental compositions of multicomponent NMP NWs (for example, binary PdP, ternary PdAgP and PdPtP NWs). With synergistically structural and compositional merits, ultrathin PdCuP NWs display dramatically enhanced ethanol electrooxidation performance with a superior mass activity of 6.7 A mgPd^{-1}, which is 9.4 fold higher than commercial Pd nanoparticle catalyst and also surpasses previously reported nanocatalysts. This approach will provide a new access for rational design of anisotropic non-metal-alloyed multicomponent noble metal-based nanocatalysts with desirable functions and synergies for a wide range of (electro)catalytic applications.

1. Introduction

One-dimensional (1D) noble metal nanowires (NWs) have received increasing attention as the highly efficient nanocatalysts for an array of applications [1–8]. In comparison to 0D isotropic nanoparticle (NP) catalysts, structural anisotropy of 1D NWs not only boosts the mass activity by facilitating the electron/mass transfer and enlarging the utilization efficiency (UE) of expensive noble metals, but also enhances the stability by decreasing Ostwald ripening and inherent dissolution processes during the (electro)catalysis. Furthermore, when downsizing the NW nanocatalysts to have an ultrathin diameter of 1–3 nm, the (electro)catalytic performances would be further improved on the basis of a surface contraction effect [9–13]. For example, the electrocatalytic performance of 1.3-nm-thick Pt NWs is 7.0 fold higher than that of commercial Pt catalyst in oxygen reduction reaction [9], and 3-nm-thick Pd NWs exhibited better activity, 2.8 fold higher than that of commercial Pd catalyst, in formic acid oxidation reaction [13].

Apart from NW nanostructure, the incorporation of other cheaper and functional elements into noble metal-based nanocatalysts to fabricate multicomponent nanoalloys would also optimize and boost their (electro)catalytic performance, and meanwhile enlarge the UEs of noble metals for various applications [7,14–21]. For instance, electrocatalytic activity in ethanol oxidation reaction (EOR) can be effectively improved by alloying more oxophilic secondary metals (Au, Ag, Cu, et. al.) with Pd/Pt based on well-known bifunctional and electronic effects [21–27]. Recently, alloying non-metals into Pd/Pt nanocatalysts becomes a hot research topic to modify the (electro)catalytic activity [7,14,28]. Introduction of non-metals, for example phosphorus (P) with abundant valence electrons, into noble metal-based nanocatalysts would remarkably modulate the electronic/geometric features, and thus boost the resultant electrocatalytic performance accordingly [23,29–33]. Inspired by the above discussions, therefore, a high-performance nanocatalyst can be rationally anticipated by combining positive synergy of anisotropic nanostructure (ultrathin NW) and ternary metal/non-metal alloy composition (for example, noble metal of Pd, oxophilic metal of Cu and non-metal of P). Unfortunately, current

---

nanosynthesis strategy is largely unsuccessful in fabricating anisotropic 1D multicomponent noble metal-phosphorus (NMP) alloy NWs. This may be ascribed to the complexity and uncertainty of the nanosynthesis in alloying amorphous P within NM nanocrystals by P-containing reducing agents (NaH_2PO_2 or $NH_4H_2PO_2$) while simultaneously nanoconfining crystalline growth of thermodynamically unfavorable 1D NWs. Therefore, it is exceedingly desirable to develop a facile and powerful synthetic methodology to prepare anisotropic ultrathin multicomponent NMP NWs and further investigate their structural and compositional synergy in optimizing electrocatalytic EOR performance.

In current work, a facile one-pot aqueous synthesis is demonstrated to directly fabricate anisotropic 1D NMP alloy NWs, for the first time. By co-reduction and crystallization of metal precursors (Pd and Cu, and/or others) with NaH_2PO_2 (as a reducing agent and a P source simultaneously) along columnar mesophases assembled by amphiphilic dioctadecyldimethylammonium chloride (DODAC), ultrathin 1D PdCuP NWs with an average diameter of 2.5 nm and length of hundreds of nanometers are successfully synthesized. DODAC with two strong hydrophobic tails as the surfactant template and under optimal reduction kinetics of NaH_2PO_2 co-play the critical roles in nanoconfining the anisotropic growth of thermodynamically unstable PdCuP NWs. Furthermore, the synthetic strategy is also adapted to tailor the P contents in PdCuP NWs (from 0 to 20 at. %) and to broad the elements in various multicomponent NMP NWs (for example, binary PdP, ternary PdAgP and PdPtP NWs). Resultant PdCuP NWs feature synergistically structural and compositional enhancement effects, and thus effectively boost their electrocatalytic EOR performance, with respect to its counterparts and commercial Pd NP catalysts.

2. Results and discussion

In a typical synthesis of ultrathin PdCuP alloy NWs, metal precursors (H_2PdCl_4 and $Cu(NO_3)_2$) were totally dissolved into an aqueous solution of DODAC. Then, PdCuP NWs were synthesized by injecting fresh-prepared NaH_2PO_2 as the reducing agent and P source under gentle shaking and keeping undisturbedly at 95 °C for 2 h (see Experimental in Supplementary Material for more details). Successful formation of ultrathin PdCuP alloy NWs with a high purity and homogeneity was clearly displayed by transmission electron microscopy (TEM). As shown in Fig. 1a and b, 1D NWs are ultrathin and partially interconnected with an average ultrathin diameter of 2.5 nm and ultralong length of hundreds of nanometers (see Fig. S1 for more TEM images). The selected-area electron diffraction (SAED) indicated PdCuP NWs have face-centered cubic (fcc) structure. High-resolution high-angle annular dark-field scanning TEM (HAADF-STEM) image further showed the lattice fringes with a *d*-spacing of 0.219 nm (Fig. 1c), indexed to (111) plane of fcc alloy nanocrystals. Slightly disordered lattices were also seen, which were ascribed to amorphous P dispersed in PdCuP NWs, as observed in PdP and PdNiP NPs [23,29,34]. Compositional alloys were further investigated using energy-dispersive X-ray spectroscopy (EDS) mapping under STEM mode, in which all elements (Pd, Cu and P) are homogeneously distributed over the whole NWs (Fig. 1d). This implied that resultant PdCuP NWs are compositionally alloyed with a uniform and spatial elemental distribution. The atomic ratio of Pd/Cu/P is determined to be 36:54:10 based on EDS analysis (Fig. S2), close to the ones obtained from X-ray photoelectron spectroscopy (XPS) and inductively coupled plasma atomic emission spectroscopy (ICP-AES).

Ultrathin PdCuP alloy NWs were further investigated by wide-angle X-ray diffraction (XRD) (Fig. 2). Five typical XRD peaks located at 40.1°, 46.7°, 68.1°, 82.1°, and 86.6°, which were ascribed to fcc Pd nanocrystals, were seen for Pd NWs. By contrast, the broader peaks with a slight shift to the lower angles in PdP NWs indicated that alloying amorphous P into Pd NWs crystallographically expanded Pd lattices [23,29]. No other set of peaks appeared, further confirming the formation of binary PdP alloys, rather than phase-separated impurities.

Similar shifts in XRD peaks were also observed in PdCu and PdCuP NWs, further implying the successful synthesis of ternary PdCuP alloy NWs.

Structural and compositional characterizations corroborated the first successful synthesis of anisotropic 1D PdCuP alloy NWs with the ultrathin size (2.5 nm) and ultralong length (hundreds of nanometer). We reasoned that both DODAC as the template and NaH_2PO_2 as the reducing agent and P source contributed cooperatively to the formation of thermodynamically unfavorable PdCuP alloy NWs. First, amphiphilic DODAC co-assembled with metal precursors into columnar hybrid mesomicelles [11]. After the injection of NaH_2PO_2 under optimal synthetic conditions, metal precursors were co-reduced into PdCu nanocrystals and simultaneously amorphous P was randomly alloyed to form ternary PdCuP. Thanks to strong hydrophobic effect of DODAC which chemically has two C_{18} tails, the crystallization growth of PdCuP alloy was nanoconfined along columnar mesophases assembled by DODAC, and thus kinetically directed in-the-columnar epitaxial growth into anisotropic ultrathin 1D NWs (Fig. S3a). The in-the-columnar epitaxial growth was also revealed by time-dependent structural evolutions, in which the length of PdCuP alloy NWs gradually grew from 5 nm (2 min), to 20 nm (10 min), and finally to > 100 nm (2 h) (Fig. S3b–e). To further highlight the importance of DODAC and optimal reduction kinetics of NaH_2PO_2, we designed a series of control experiments for comparisons.

First, the surfactants with the same chemical structures of DODAC but with the shorter hydrophobic alkyl chains (including dihexadecyldimethylammonium chloride (C_8), didodecyldimethylammonium chloride (C_{12}), and dioctyldimethylammonium chloride (C_{16})) were checked under the same synthesis conditions (Fig. S4). Only irregular NPs could be formed by the surfactants with the shorter hydrophobic chains (C_8 and C_{12}), while short NWs were obtained in the C_{16} surfactant. These results definitely indicated that the strong hydrophobicity of DODAC could nanoconfine the crystalline growth of PdCuP NWs along the surfactant template. Moreover, the nanosynthesis was also carried out in the absence of surfactant or in the presence of most-used surfactant ligand of polyvinylpyrrolidone (PVP) [7]. Irregular NPs were obtained (Fig. S5a–d), suggesting the disability of the synthetic conditions for PdCuP NWs. The surfactant of octadecyltrimethylammonium chloride (C_{18}TAC) which contains only one hydrophilic C_{18} tail and a quaternary ammonium head was also investigated. Partially attached NPs instead of ultrathin NWs were obtained (Fig. S5e, f), indicating the nanoconfinement effect of C_{18}TAC failed to engineer in-the-columnar growth of PdCuP nanocrystals, although columnar mesostructure may be formed [35,36]. The NP aggregates could evolve into short nanorods (5–20 nm) when behenyltrimethylammonium chloride (C_{22}TAC) with a longer hydrophobic tail was used (Fig. S5g, h). Besides, bifunctional carbonyl and quaternary ammonium groups in the surfactant [37] cannot direct in the formation of ultrathin NWs (Fig. S5i, j), also implying the role of DODAC. The concentration of DODAC in aqueous solution was also changed to investigate the effect for the formation of 1D PdCuP NWs, in which the low concentration of DODAC resulted in short PdCuP NWs (Fig. S6). These observations further confirmed that strong hydrophobicity of DODAC is structurally vital in nanoconfining in-the-columnar epitaxial growth of ultrathin PdCuP NWs along assembled columnar mesophases.

Second, the reduction kinetics of NaH_2PO_2 as reducing agent and P source was studied by optimizing pH and temperature of reaction solution, as it is critical in controlling the nanostructures of PdCuP alloys. We found ultrathin PdCuP NWs were obtained in the pH range of 7.13 and 10.80 and under the reaction temperature range of 75–120 °C (Figs. S7 and S8). Both the lower pH and higher temperature promoted the reduction kinetics, and thus gave rise to small NPs (Figs. S7a, b and S8i, j). By contrast, the shorter NWs or their aggregates were obtained in the higher pH and lower temperature (Figs. S7g, h and S8a, b), indicating the slower reduction rate facilitated the formation of thermodynamically more stable nanostructures. These results definitely
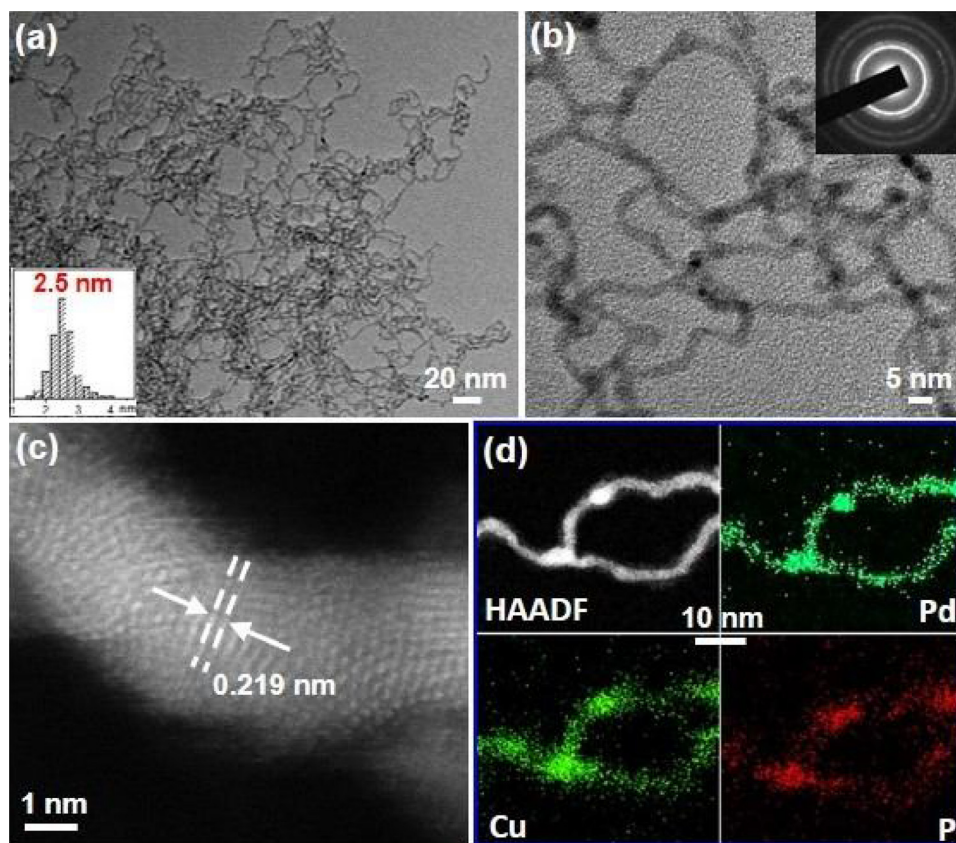
Fig. 1. (a) Low-magnification, (b) high-magnification TEM, (c) high-resolution HAADF-STEM images, and (d) elemental mappings of ultrathin ternary PdCuP alloy NWs. Inset in (b) is SAED pattern of PdCuP NWs.
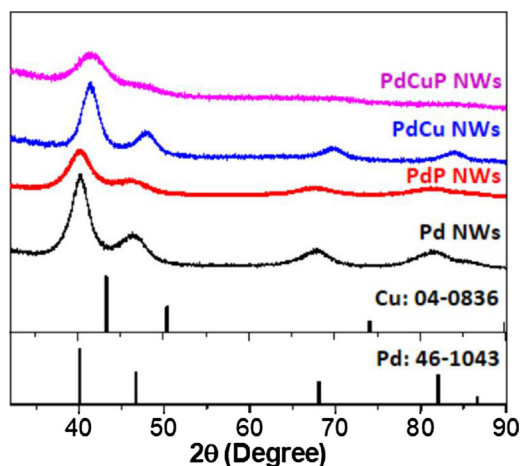

Fig. 2. Wide-angle XRD patterns of ultrathin PdCuP, PdCu, PdP and Pd NWs.

suggested the importance of optimal reduction kinetics of NaH_2PO_2 in the synthesis of ultrathin PdCuP alloy NWs.

Our synthetic protocol is pretty universal and can be extended to precisely tailor elemental ratios and compositions of NMP alloy NWs. Taking PdCuP as an example, we found P content in PdCuP alloys can be precisely tailored in the range of 3 and 20 at.% by changing initial feed ratios (P amounts). All the PdCuP alloys with P content of > 3 at. % are structurally 1D NWs (Figs. 3b–d and S9), despite the higher P content resulted in the shorter and aggregated ones (Fig. 3d). Similarly, elemental ratios of Pd/Cu in PdCuP NWs were also controlled (Fig. S10). The tunability in compositional ratios of PdCuP NWs is important to optimize surface electronic states and functions as well as electrocatalytic performance (see below). Besides, we also investigated the

synthetic strategy in tuning elemental compositions in other ultrathin multicomponent NMP NWs. We found, not only 3d metal of Cu, but also 4d metal of Ag and 5d metal of Pt can be successfully alloyed into ultrathin NMP NWs. As shown in Fig. 3e–g, binary PdP, ternary PdAgP and PdPtP alloy NWs were obtained, due to nanoconfinement effect of DODAC (also see Fig. S11–13). Among them, PdAgP NWs are slightly thicker, possibly because of the quicker crystallization rate of Ag^+/Ag [24,38]. All above observations further confirmed the synthetic capacity of our method in nanoengineering ultrathin multicomponent NMP alloy NWs.

Electrocatalytic EOR was investigated as a model reaction to evaluate catalytic performance of ultrathin ternary PdCuP alloy NWs (Fig. 1), and the results were also compared to its counterparts with the same NW nanostructure (PdP NWs in Fig. 3e, PdCu and Pd NWs in Fig. S14) and composition (PdCuP NPs in Fig. S6e) as well as commercial Pd NPs. Before activity tests, we first studied the electrochemical active surface areas (ECSAs) of all the nanocatalysts from oxygen desorption peaks of cyclic voltammograms (CVs) in 1.0 M KOH (Fig. 4a). Notably, PdCuP NWs showed the highest ECSA of $69.2\,m^2\,g_{Pd}^{-1}$, which is 1.3–2.8 times larger than its counterparts and 7.2 times than Pd NPs (Fig. 4b). This indicated that PdCuP NWs exposed the highest active sites for EOR due to its ultrathin NW nanostructure and ternary alloy composition. Fig. 4c shows the CVs in 1.0 M KOH and 1.0 M ethanol, indicating all above nanocatalysts are electrocatalytically active for the EOR. The mass activity of PdCuP, PdP, PdCu and Pd NWs, PdCuP NPs and Pd NPs is 6.67, 3.02, 2.95, 2.01, 3.74 and 0.71 A mg_{Pd}^{-1}, respectively (Fig. 4d). Obviously, ultrathin ternary PdCuP NWs displayed remarkably enhanced EOR activity than its NW and NP counterparts, and is also superior to previously reported state-of-the-art nanocatalysts (Table S1) [21,23,24]. We also investigated the EOR activity of ultrathin PdCuP NWs with different compositional ratios (Fig. S15–16); "volcano"-type mass activity further implied an optimal compositional
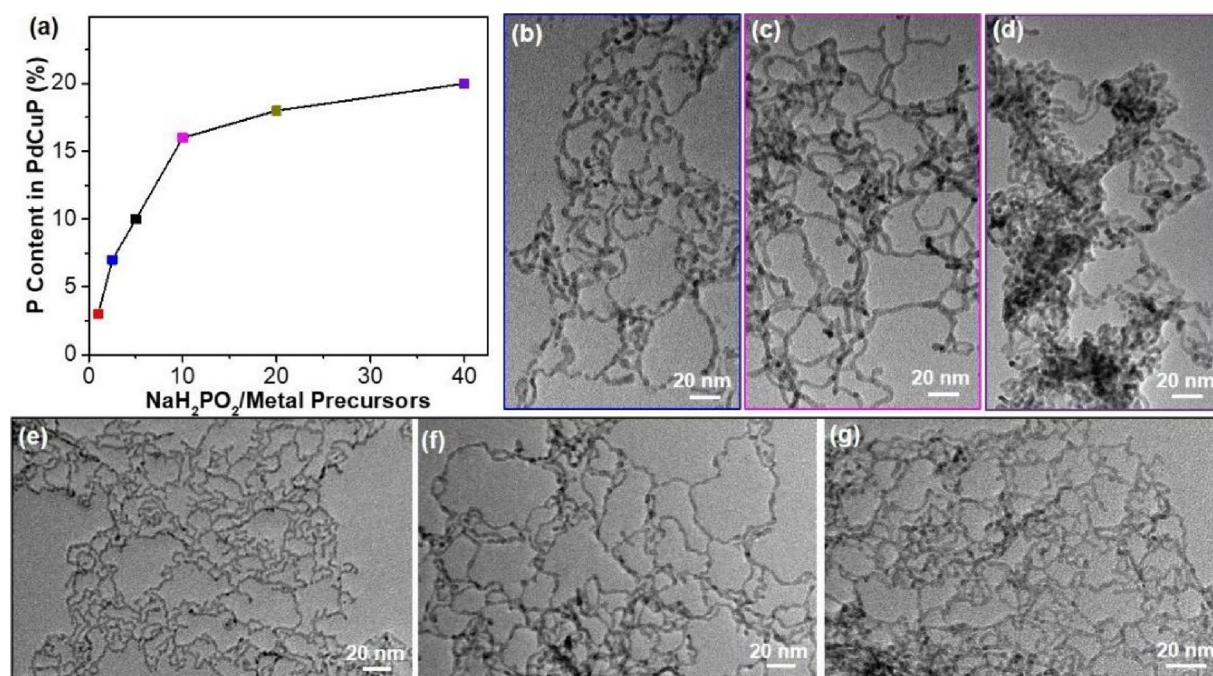
Fig. 3. (a) Elemental "phase-like" diagram and (b–d) typical TEM images of PdCuP NWs with different P contents. Typical TEM images of (e) PdP, (f) PdAgP, and (g) PdPtP NWs.

effect of PdCuP NWs in the electrocatalysis.

To reveal how and why ternary PdCuP NWs improved EOR activity, high-resolution XPS analysis was carried out to investigate the chemical states of Pd, Cu, and P by comparing PdCu and PdCuP alloy NWs. Two pairs of XPS Pd 3d peaks can be deconvoluted for both PdCu and PdCuP NWs, in which major Pd^0 suppressed minor Pd^{2+} species (Fig. 5a). The $3d_{5/2}$ peak of Pd^0 in PdCuP alloy NWs is located in 335.40 eV, 0.28 eV

negatively shifted than that of PdCu NWs (335.68 eV), indicating alloying P within PdCu downshifted the Fermi level of Pd due to the strong electronic interactions involving Pd, Cu and P [23]. Optimal Fermi level would weaken the adsorption of the intermediates and reactants on Pd, thus improving EOR performances accordingly [39,40]. Meanwhile, compared to Cu 2p in PdCu NWs, only few nominally reduced Cu^0 was seen in PdCuP NWs (Fig. 5b). Dominant presence of
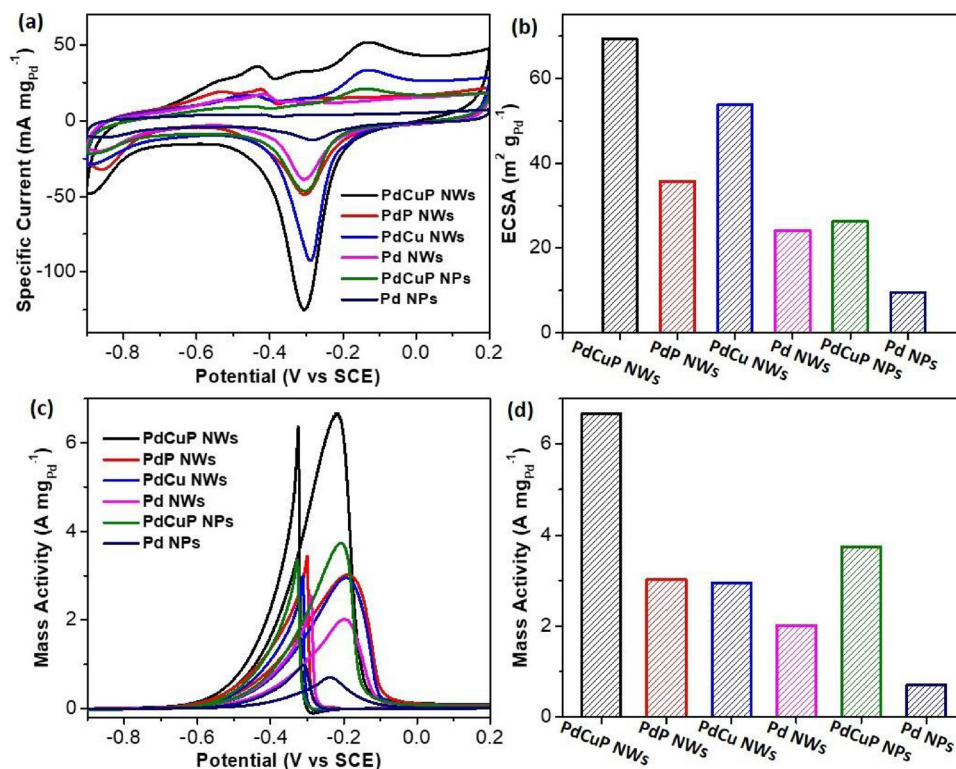

Fig. 4. (a) CV curves and (b) summarized ECSAs of ultrathin PdCuP, PdP, PdCu, and Pd NWs, PdCuP NPs and commercial Pd NPs in 1.0 M KOH. (c) CV curves and (d) summarized mass activities of ultrathin PdCuP, PdP, PdCu, and Pd NWs, PdCuP NPs and commercial Pd NPs in 1.0 M KOH and 1.0 M ethanol.
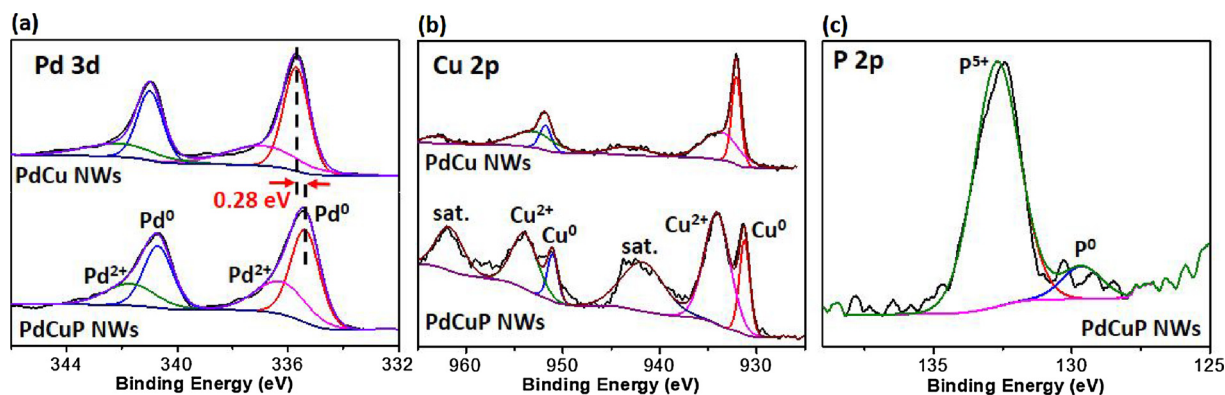
Fig. 5. High-resolution XPS spectra of (a) Pd 3d, (b) Cu 2p, and (c) P 2p of PdCuP and PdCu NWs.

Cu^{2+} and sat. $(Cu(OH)_2)$ species in ternary PdCuP NWs suggests that oxygen (O) favors to adsorb on the surface Cu sites by the formation of Cu-P, as previously observed in PdNiP alloys [23,40]. Ideally, the favorable adsorption in O-containing species $(Cu-OH_{ads})$ could accelerate the further oxidation of the CO_{ads} and CH_3CO_{ads}, and further correspond to enhanced performance in electrocatalytic EOR [23,24,38]. Furthermore, high-resolution P 2p spectrum in PdCuP NWs was revealed, where the peaks at 132.7 and 129.6 eV are ascribed to the oxidized P^{5+} (P_2O_5) and elemental state P^0 species, respectively (Fig. 5c). Also, a negative shift of 0.7 eV in the binding energy (P^0) can be distinguished for PdCuP NWs than that for red phosphorus, implying that elemental P^0 species accept partial electrons from surrounding metals of Pd and Cu into oxidized P^{5+} [23,34,40].

Based on the above discussions, we can ascribe remarkable EOR activity of ultrathin PdCuP NWs to synergic enhancement effect of structural and compositional advantages (Fig. 6). On one hand, structurally ultrathin NWs would expose more electrochemical active sites and also facilitate the mass/electron transfer during the electrocatalysis. On the other hand, ternary chemical elements alloyed with metal of Cu and non-metal of P could weaken the adsorption of the intermediates $(CO_{ads}$ and $CH_3CO_{ads})$ by modifying the electronic state of Pd, and also optimize the further removal /oxidation of above poisoning intermediates by promoting the formation of OH_{ads} (Cu-OH_{ads} and P-OH_{ads}). Both of them would accelerate the electrocatalytic kinetics and thus enhance electrocatalytic performance in EOR.

The decreased adsorption energy and accelerated electrocatalytic

kinetics of ultrathin PdCuP NWs were experimentally depicted by both more negative onset potential and higher I_f/I_b (the ratio of forward and backward peak current) value from the CVs (Fig. 7a) [24,25]. Meanwhile, we also compared the activities of above nanocatalysts at different scan rates (Fig. S17) and ethanol concentrations (Fig. S18), further indicating enhanced electrocatalytic kinetics by ultrathin PdCuP NWs. Such deductions were also confirmed by imitating CO anti-poisoning tests. As shown in Fig. 7b, ultrathin ternary PdCuP NWs displayed the largest surface area and lowest potential with respect to its counterparts, indicating superior capacity for the removal of CO_{ads} on the nanocatalysts [21,23,34]. These results definitely confirmed the positive synergy of structural (ultrathin NW) and compositional (ternary PdCuP) merits in accelerating the electrocatalytic kinetics and enhancing EOR activity. Lastly, structural anisotropy and compositional ternary alloy of PdCuP NWs also dramatically improved the electrocatalytic stability (Figs. 7c and S19), because the nanocatalysts alleviated Oswald ripening and dissolution processes and facilitated the removal of poisoning intermediates [5,7,11].

3. Conclusions

In conclusion, we presented a straightforward one-pot aqueous synthesis approach to preparing ternary NMP alloy NWs, for the first time. The NMP NWs featured ultrathin diameter (2.5 nm) and ultralong length (hundreds of nanometers) as well as ternary alloy compositions. Such anisotropic 1D nanostructure was achieved by in-the-columnar epitaxial growth of PdCuP alloy NWs along nanoconfined mesomicelles assembled by DODAC using NaH_2PO_2 as the reducing agent and P source under optimal conditions. Furthermore, the synthetic strategy can be extended to control the elemental ratios of PdCuP NWs, and to synthesize other ultrathin NMP alloy NWs. Because of the positive synergy of structural and compositional features which modified the electron state of Pd and facilitated the removal of poisoning intermediates, ultrathin ternary PdCuP NWs exhibited remarkably improved EOR activity and stability, with respect to its counterparts and previously reported nanocatalysts. We believe that the synthetic strategy for ultrathin NMP alloy NWs could be readily adapted to fabricate libraries of anisotropic NMP alloy nanocatalysts with synergic enhancement effect for a broad range of (electro)catalytic applications.
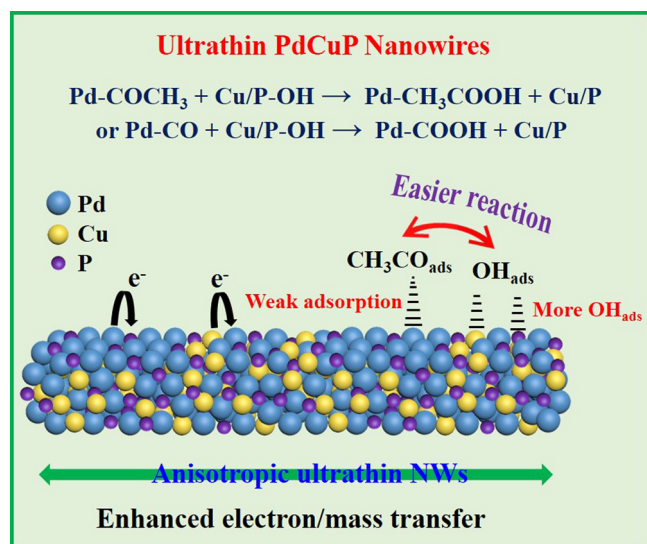
Fig. 6. Schematic illustrating the electrocatalytic EOR of ultrathin ternary PdCuP alloy NWs.
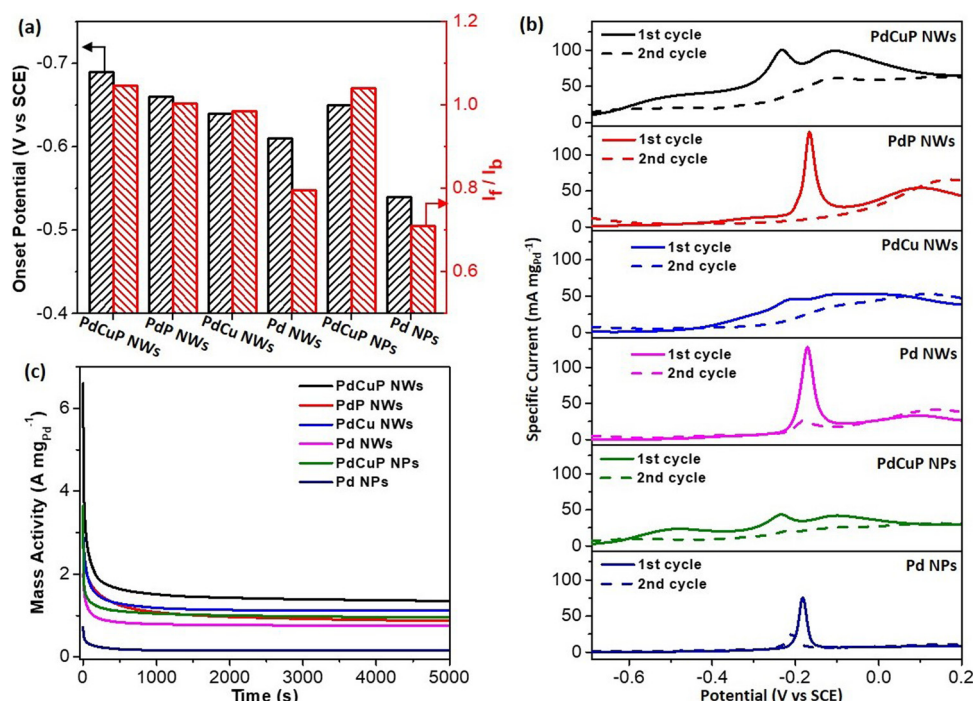
Fig. 7. (a) Electrocatalytic kinetics (onset potential and I_f/I_b), (b) CO-stripping voltammograms, and (c) i–t chronoamperometry curves of ultrathin PdCuP, PdP, PdCu, and Pd NWs, PdCuP NPs and commercial Pd NPs.

Appendix A. Supplementary data

Supplementary material related to this article can be found, in the online version, at doi:https://doi.org/10.1016/j.apcatb.2019.04.066.

References

[1] H. Li, S. Zhao, M. Gong, C. Cui, D. He, H. Liang, L. Wu, S. Yu, Ultrathin PtPdTe nanowires as superior catalysts for methanol electrooxidation, Angew. Chem. Int. Ed. 52 (2013) 7472–7476.

[2] S. Guo, D. Li, H. Zhu, S. Zhang, N. Markovic, V. Stamenkovic, S. Sun, FePt and CoPt nanowires as efficient catalysts for the oxygen reduction reaction, Angew. Chem. Int. Ed. 52 (2013) 3565–3468.

[3] C. Zhu, S. Guo, S. Dong, PdM (M = Pt, Au) bimetallic alloy nanowires with enhanced electrocatalytic activity for electro-oxidation of small molecules, Adv. Mater. 24 (2012) 2326–2331.

[4] W. Wang, F. Lv, B. Lei, S. Wan, M. Luo, S. Guo, Tuning nanowires and nanotubes for efficient fuel-cell electrocatalysis, Adv. Mater. 28 (2016) 10117–10141.

[5] Y. Lu, S. Du, R. Steinberger-Wilckens, One-dimensional nanostructured electro-catalysts for polymer electrolyte membrane fuel cells-a review, Appl. Catal. B-Environ. 199 (2016) 292–314.

[6] G. Chen, C. Xu, X. Huang, J. Ye, L. Gu, G. Li, Z. Tang, B. Wu, H. Yang, Z. Zhao, Interfacial electronic effects control the reaction selectivity of platinum catalysts, Nat. Mater. 15 (2016) 564.

[7] Z. Liu, J. Qi, M. Liu, S. Zhang, Q. Fan, H. Liu, K. Liu, H. Zheng, Y. Yin, C. Gao, Aqueous synthesis of ultrathin platinum/non-noble metal alloy nanowires for en-hanced hydrogen evolution activity, Angew. Chem. Int. Ed. 57 (2018) 11678–11682.

[8] M. Li, Z. Zhao, T. Cheng, A. Fortunelli, C. Chen, R. Yu, Q. Zhang, L. Gu, B. Merinov, Z. Lin, Ultrafine jagged platinum nanowires enable ultrahigh mass activity for the oxygen reduction reaction, Science 354 (2016) 1414–1419.

[9] C. Koenigsmann, W. Zhou, R. Adzic, E. Sutter, S. Wong, Size-dependent enhance-ment of electrocatalytic performance in relatively defect-free, processed ultrathin platinum nanowires, Nano Lett. 10 (2010) 2806–2811.

[10] L. Zhang, N. Li, F. Gao, L. Hou, Z. Xu, Insulin amyloid fibrils: an excellent platform for controlled synthesis of ultrathin superlong platinum nanowires with high elec-trocatalytic activity, J. Am. Chem. Soc. 134 (2012) 11326–11329.

[11] H. Lv, X. Chen, D. Xu, Y. Hu, H. Zheng, S.L. Suib, B. Liu, Ultrathin PdPt bimetallic nanowires with enhanced electrocatalytic performance for hydrogen evolution re-action, Appl. Catal. B-Environ. 238 (2018) 525–532.

[12] L. Cademartiri, G. Ozin, Ultrathin nanowires-a materials chemistry perspective, Adv. Mater. 21 (2009) 1013–1020.

[13] D. Xu, X. Liu, M. Han, J. Bao, Facile synthesis of ultrathin single-crystalline palla-dium nanowires with enhanced electrocatalytic activities, Chem. Commun. 52 (2016) 12996–12999.

[14] T. Vo Doan, J. Wang, K. Poon, D. Tan, B. Khezri, R. Webster, H. Su, H. Sato, Theoretical modelling and facile synthesis of a highly active boron-doped palladium catalyst for the oxygen reduction reaction, Angew. Chem. Int. Ed. 55 (2016) 6842–6847.

[15] Y. Yao, Z. Huang, P. Xie, S. Lacey, R. Jacob, H. Xie, F. Chen, A. Nie, T. Pu, M. Rehwoldt, Carbothermal shock synthesis of high-entropy-alloy nanoparticles, Science 359 (2018) 1489–1494.

[16] Z. Seh, J. Kibsgaard, C. Dickens, I. Chorkendorff, J. Nørskov, T. Jaramillo, Combining theory and experiment in electrocatalysis: insights into materials design, Science 355 (2017) eaad4998.

[17] M. Luo, S. Guo, Strain-controlled electrocatalysis on multimetallic nanomaterials, Nat. Rev. Mater. 2 (2017) 17059.

[18] C. Bianchini, P. Shen, Palladium-based electrocatalysts for alcohol oxidation in half cells and in direct alcohol fuel cells, Chem. Rev. 109 (2009) 4183–4206.

[19] J. Greeley, M. Mavrikakis, Alloy catalysts designed from first principles, Nat. Mater. 3 (2004) 810–815.

[20] L. Bu, N. Zhang, S. Guo, X. Zhang, J. Li, J. Yao, T. Wu, G. Lu, J. Ma, D. Su, Biaxially strained PtPb/Pt core/shell nanoplate boosts oxygen reduction catalysis, Science 354 (2016) 1410–1414.

[21] J. Hong, Y. Kim, D. Wi, S. Lee, S. Lee, Y. Lee, S. Choi, S. Han, Ultrathin free-standing ternary-alloy nanosheets, Angew. Chem. Int. Ed. 55 (2016) 2753–2758.

[22] Y. Wang, G. Wang, G. Li, B. Huang, J. Pan, Q. Liu, J. Han, L. Xiao, J. Lu, L. Zhuang, Pt-Ru catalyzed hydrogen oxidation in alkaline media: oxophilic effect or electronic effect? Energy Environ. Sci. 8 (2015) 177–181.

[23] L. Chen, L. Lu, H. Zhu, Y. Chen, Y. Huang, Y. Li, L. Wang, Improved ethanol elec-trooxidation performance by shortening Pd–Ni active site distance in Pd-Ni-P na-nocatalysts, Nat. Commun. 8 (2017) 14136.

[24] H. Lv, A. Lopes, D. Xu, B. Liu, Multimetallic hollow mesoporous nanospheres with synergistically structural and compositional effects for highly efficient ethanol electrooxidation, ACS Cent. Sci. 4 (2018) 1412–1419.

[25] Y. Yang, L. Jin, B. Liu, P. Kerns, J. He, Direct growth of ultrasmall bimetallic aupd nanoparticles supported on nitrided carbon towards ethanol electrooxidation, Electrochim. Acta 269 (2018) 441–451.

[26] U. Demirci, Theoretical means for searching bimetallic alloys as anode electro-catalysts for direct liquid-feed fuel cells, J. Power Sources 173 (2007) 11–18.

[27] H. Lv, Y. Wang, A. Lopes, D. Xu, B. Liu, Ultrathin PdAg single-crystalline nanowires enhance ethanol oxidation electrocatalysis, Appl. Catal. B-Environ. 249 (2019) 116–125.

[28] K. Jiang, K. Xu, S. Zou, W. Cai, B-doped Pd catalyst: boosting room-temperature hydrogen production from formic acid-formate solutions, J. Am. Chem. Soc. 136 (2014) 4861–4864.

[29] H. Yang, Z. Yu, S. Li, Q. Zhang, J. Jin, J. Ma, Ultrafine palladium-gold-phosphorus ternary alloyed nanoparticles anchored on ionic liquids-noncovalently functiona-lized carbon nanotubes with excellent electrocatalytic property for ethanol oxida-tion reaction in alkaline media, J. Catal. 353 (2017) 256–264.

[30] J. Zhang, Y. Xu, B. Zhang, Facile synthesis of 3D Pd-P nanoparticle networks with enhanced electrocatalytic performance towards formic acid electrooxidation, Chem. Commun. 50 (2014) 13451–13453.

[31] F. He, K. Li, C. Yin, Y. Wang, M. Jiao, H. Tang, Z. Wu, A first-principles study on the effect of phosphorus-doped palladium catalyst for formic acid dissociation, Appl. Surf. Sci. 387 (2016) 221–227.

[32] J. Chang, L. Feng, C. Liu, W. Xing, X. Hu, An effective Pd-Ni$_2$P/C anode catalyst for direct formic acid fuel cells, Angew. Chem. Int. Ed. 53 (2014) 122–126.

[33] P. Mei, J. Kim, N.A. Kumar, M. Pramanik, N. Kobayashi, Y. Sugahara, Y. Yamauchi, Phosphorus-based mesoporous materials for energy storage and conversion, Joule 2 (2018) 2289–2306.

[34] L. Zhang, D. Lu, Y. Chen, Y. Tang, T. Lu, Facile synthesis of Pd-Co-P ternary alloy network nanostructures and their enhanced electrocatalytic activity towards hydrazine oxidation, J. Mater. Chem. A 2 (2014) 1252–1256.

[35] Y. Guan, M. Antonietti, C. Faul, Ionic self-assembly of dye-surfactant complexes: influence of tail lengths and dye architecture on the phase morphology, Langmuir 18 (2002) 5939–5945.

[36] J. Shen, X. Xin, G. Liu, J. Pang, Z. Song, G. Xu, S. Yuan, Fabrication of smart pH-responsive fluorescent solid-like giant vesicles by ionic self-assembly strategy, J. Phys. Chem. C 120 (2016) 27533–27540.

[37] D. Xu, X. Liu, H. Lv, Y. Liu, S. Zhao, M. Han, J. Bao, J. He, B. Liu, Ultrathin palladium nanosheets with selectively controlled surface facets, Chem. Sci. 9 (2018) 4451–4455.

[38] H. Lv, L. Sun, L. Zou, D. Xu, H. Yao, B. Liu, Size-dependent synthesis and catalytic activities of trimetallic PdAgCu mesoporous nanospheres in ethanol electrooxidation, Chem. Sci. 10 (2019) 1986–1993.

[39] L. Kibler, A. El-Aziz, R. Hoyer, D. Kolb, Tuning reaction rates by lateral strain in a palladium monolayer, Angew. Chem. Int. Ed. 44 (2005) 2080–2084.

[40] Y. Wang, F. Shi, Y. Yang, W. Cai, Carbon supported Pd-Ni-P nanoalloy as an efficient catalyst for ethanol electro-oxidation in alkaline media, J. Power Sources 243 (2013) 369–373.